TÜBİTAK

Turkish Journal of Zoology

http://journals.tubitak.gov.tr/zoology/

Research Article

Turk J Zool
(2019) 43:
© TÜBİTAK
doi:10.3906/zoo-1809-21

A study on European anchovy (*Engraulis encrasicolus*) swimbladder with some considerations on conventionally used target strength

Meltem OK*, **Ali Cemal GÜCÜ**
Institute of Marine Sciences, Middle East Technical University, Erdemli, Mersin, Turkey

Received: 17.09.2018 • **Accepted/Published Online:** 31.01.2019 • **Final Version:** 00.00.2019

Abstract: Hydroacoustic surveys are one of the prime methods to assess the commercially top-ranked small pelagic stocks. The method relies on acoustic scattering from a fish, which is largely controlled by the size and morphology of the swimbladder. In this study, the changes in the size of the European anchovy swimbladder sampled in the Black Sea were investigated. Ventral cross-sectional area (by photographing the ventrally dissected fish) and volume (by dorsal and lateral X-raying) of the swimbladders were estimated. Comparison of areas showed that the stomach fill and presence of viscera did not have a statistically significant impact on the swimbladder size while the hepatosomatic index showed significant impact. Although the vertical distribution of the anchovy is naturally not very wide due to absence of sufficient oxygen below 100 m, sampling depth showed significant impact on the volume of the swimbladder. However, it was also observed during X-ray imaging that a considerable number of fish (87%) had deflated swimbladders. The reasons for this variability, which may have significant implication on the acoustic estimations and stock assessment, were also discussed. The importance of acclimatization of the fish at surface conditions in studies addressing changes in swimbladder morphometry was underlined.

Key words: European anchovy, swimbladder, hydroacoustics, target strength, Black Sea

1. Introduction

Effective quantification of the distribution and abundance of small pelagic fish such as anchovy and sardines is generally carried out by means of hydroacoustic studies (Simmonds and MacLennan, 2005). In principle, the method relies on integration of the echo intensity reflected by acoustically detectable fish schools (MacLennan, 1990). At this end, target strength (TS), a measure of the backscattering capacity of fish, is a fundamental parameter required to convert the backscattering intensity to fish density (MacLennan, 1990). On the other hand, what determines the backscattering capacity of a fish is, to a great extent, is its swimbladder, which is reported to be responsible for 90%–95% of the target strength (Foote, 1980). Theoretical computations based on the exact form of the swimbladder (Foote, 1985; Foote and Ona, 1985) further demonstrated that the shape as well as the size of the swimbladder is important for the acoustic reflection. Therefore, any changes in the swimbladder volume and shape may influence quantitative estimates of fish abundance (Foote, 1980; Blaxter and Batty, 1990; Zhao et al., 2008).

Another important aspect of the TS is that, when fish are exposed to pressure changes, such as during diel vertical migrations, remarkable volume changes may occur in the swimbladder dimensions (Zhao et al., 2008; Ganias et al., 2015). These changes may be particularly important for species with closed swimbladders (physoclists), while those with open swimbladders (physostomes) may compensate ambient pressure change by releasing gas through a pneumatic duct (Blaxter et al., 1979).

Therefore, characterization and understanding of the structural morphology of the swimbladder and its relation to fish behavior is particularly important to get more accurate TS values and ultimately more accurate estimations of fish abundance (Fassler et al., 2009; Ganias et al., 2015).

Early studies to explore swimbladder morphology were mainly based on estimation of volume from the amount of gas contained in the swimbladder (Blaxter et al., 1979; Fine et al., 1995). Later, more advanced techniques were explored to model the structure of the swimbladder (Ona, 1990; Machias and Tsimenidis, 1995; Ganias et al., 2015), including noninvasive radiographic techniques such as X-ray imagery (Hazen and Horne, 2003; Yasuma et al., 2003; Robertson et al., 2008; Sawada et al., 1999; Scoulding et al., 2015), and MRI scanning (Pena and Foote, 2008; Fassler et al., 2009, 2013).

Despite the sensitivity of the swimbladder to external factors such as pressure, the conventional approach in TS

* Correspondence: meltemok@ims.metu.edu.tr

estimation is to use a single empirically defined equation approximating TS as a function of the length of the fish. This simplified approach is prone to significant variations in the hydroacoustically estimated biomass of fish.

In this study we aimed to estimate TS of the Black Sea anchovy *Engraulis encrasicolus* (Linnaeus, 1758) based on the size of the swimbladder and to compare these estimates with the conventionally estimated values. Moreover, we questioned whether the anchovy swimbladder is affected by the physiological condition of the individual.

2. Materials and methods

Anchovy samples were collected in the Black Sea during a fisheries survey carried out in November and December 2016 by the Middle East Technical University (METU) Institute of Marine Sciences (IMS) onboard the R/V Bilim-2. All samples were collected using a pelagic trawl towed at speeds of 3.5–4.5 knots for a duration of 30 min. Two different methods were used in order to explore swimbladder characteristics: i) dissection onboard and immediate measurements and photography for further image analysis to calculate the size of the ventral cross-section area of the swimbladder, and ii) X-ray measurements of anchovies immediately frozen after sampling, to calculate the swimbladder volume.

2.1. Swimbladder measurement onboard and in the laboratory

Anchovy samples were dissected, measured, and photographed onboard the R/V Bilim-2 immediately after capture by following the methodology described by Ganias et al. (2015). A total of 48 live individuals were selected for this purpose. Prior to dissection, each individual was measured for total length (TL: mm). In order to account for the possible impact of feeding state, stomach fullness (empty or full) and presence or absence of viscera (FI) of each dissected individual were macroscopically examined. As the sampling was performed outside the active reproduction period, the effect of gonad size was assumed to be insignificant and there was no difference between males and females during this period.

Later, the viscera were removed in order to avoid damaging the swimbladder and the entire cross-section of the swimbladder was investigated after fully opening the coelomic cavity. The samples with fully deflated swimbladder were excluded from the analyses due to poor visibility. Sixty-six photographs belonging to swimbladders of 16 individuals were taken for image analyses. After photographing them onboard, each specimen (eviscerated) and the gonads, liver, and stomach were frozen at –20 °C for further analyses in the laboratory. Naturally, the size of the swimbladder increases parallel to the size of the fish. This effect was removed by modeling the relationship between the body weight of the fish and the area of the swimbladder as Area = $a \times W^b$ (Graham, 2003) and the residuals of the model were used as the relative swimbladder size. The detailed examinations of swimbladder characteristics were done at the laboratory of IMS-METU by processing the digital images taken during the surveys. Olympus Stream software was used for the image analysis. The swimbladder length (mm) and the ventral cross-sectional area (mm^2) were measured after calibrating each image in the software (Figure 1). The hepatosomatic index (HSI) was calculated as liver weight to total weight ratio.

2.2. Swimbladder measurement by X-ray imaging

After defrosting the samples, X-ray image acquisition (i.e. computed radiography, CR) was performed by positioning the group of fish between the X-ray source and detector, which provided a two-dimensional projection of a three-dimensional swimbladder. In each session 18 to 27 anchovy samples (depending on the size of the individuals) were radiographed on their dorsal and lateral aspects in accordance with previous studies (Sawada et al., 1999; Yasuma et al., 2003) (Figure 2). The exposure was at 0.69 mAs for 4.3 ms at 85 kV potential. A metallic disk with known dimensions was also placed on the plate for scaling purposes.

The swimbladder volumes were calculated by using two alternative approaches, which assumed the swimbladder shape as i) a series of truncated ellipsoidal cones with two conic ellipsoid at the anterior and posterior ends and ii) a

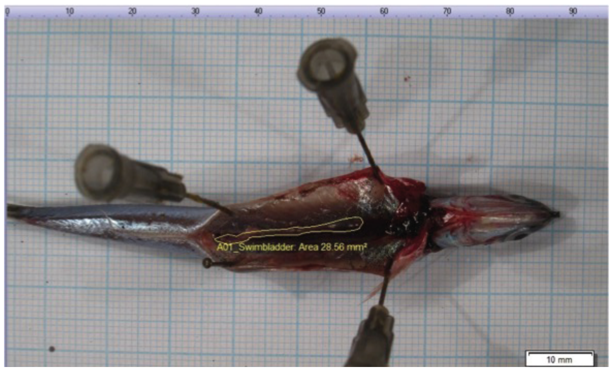

Figure 1. An example showing the postprocessing image analyses of anchovy swimbladder.

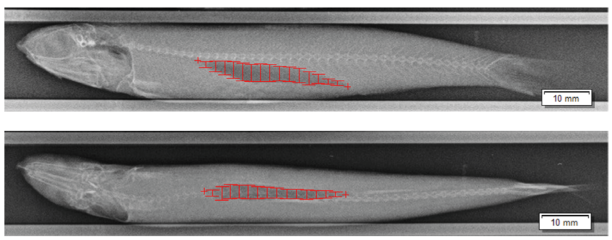

Figure 2. European anchovy (*Engraulis encrasicolus*): lateral (upper) and dorsal (lower) radiographs and the measurement steps shown on the same image. The swimbladder is the dark structure in the center of the body.

prolate spheroid shape (Capen, 1967) (Figure 3, upper and lower panel, respectively).

In the first approach, it was assumed that the volume of the swimbladder is equal to the sum of the volumes of a series of ellipsoidal truncated cones (see Figure 3, upper panel). On the X-ray images displaying the dorsal and lateral cross-sections of the swimbladder the nodes joining the vertebral bones were used as landmarks in order to properly determine the location of the cones. The distance between two perpendicular lines passing through two successive reference vertebrae on the lateral view was assumed to reflect the height (h) of truncated cone (Figure 3, upper panel). The length of the two successive vertical lines on the lateral view gives the longest radius, D2 and D4. The shortest radius of D1 and D3 was measured using the dorsal view of the same swimbladder (Figure 3, upper panel).

In the second approach proposed by Capen (1967), swimbladder volume was calculated from the formula SV = 4/π3 (a/2)(b/2)(c/2) (a: swimbladder length, b: swimbladder height, and c: swimbladder width). For both approach, the "effective radius", ER, of the swimbladder was assumed to be the radius of a sphere that has the same volume as the swimbladder, estimated by the formula ER = $V/4/3\pi^{1/3}$.

2.3. Target strength (TS) estimation

Target strength of the samples was estimated by two approaches. The first is the following conventional function suggested by ICES (1983) and commonly used in hydroacoustic anchovy biomass estimation studies (Pyrounaki et al., 2012):

TS = 20 log L – 71.2 dB, where L is the fish length in cm.

The second approach is based on the assumption that the size of the swimbladder is the dominant factor that determines the TS of a fish (Foote, 1980) and can therefore be expressed by the following relationship suggested for the TS of very small spheres (Hodges, 2010):

$$TS_{teo} = 10log\frac{1082R^6}{\lambda^4},$$

where R is the radius and λ is wavelength. For the frequency commonly used in fisheries surveys (38 kHz),

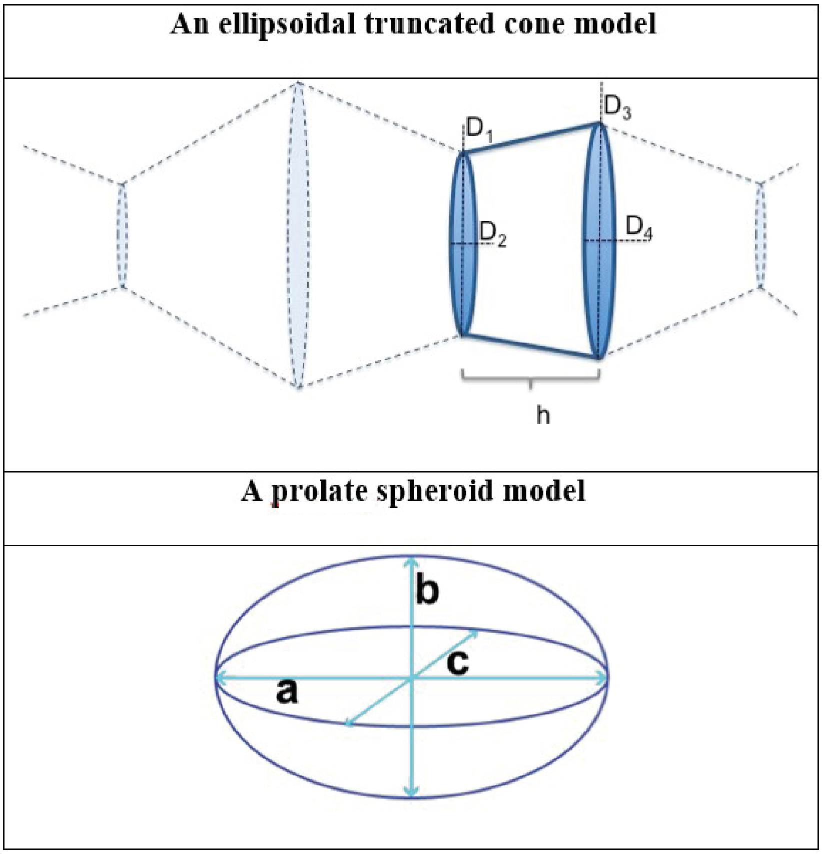

Figure 3. Definition of the landmarks corresponding to parameters of ellipsoidal truncated cones and a prolate spheroid model (hereafter "ellipsoid" and "spheroid", respectively).

λ is approximately 0.039 m. The formula has been solved for the volumes estimated with both ellipsoid and spheroid approaches and two different sets of theoretical TS series were obtained.

2.4. Statistical analysis

Effects of the physical and physiological factors on the swimbladder characteristics were analyzed using factorial ANOVA; paired data, such as volume estimates based on the two different approaches, were compared by Student's test; the relationships between variables were tested using linear models; normality was tested by QQ plot; and departure from normality was corrected by log10 transformation when applicable. All of the analyses were carried out with the statistical software R version 3.3.2 (R Core Team, 2016) and RStudio version 3.4.1 (RStudio Team, 2017).

3. Results

Of 48 anchovies dissected, sixteen possessed a swimbladder not deflated. The mean ventral cross-sectional area of the anchovies examined was 61.36 mm^2 (±17.6; 95% CI). The estimated swimbladder areas in different states showed that swimbladders with no visceral fat had the highest mean cross-sectional area, followed by anchovies with empty stomachs (Table 1). Weight and HSI of the fish had significant impact on the cross-sectional area of the swimbladder (Table 2). The depth of sampling also had a significant impact on the size of the area, while the effects of the other variables were not significant. A positive correlation was found between swimbladder area and fish size (body length) (Figure 4) and the effect of fish size was significant (Table 3). The slope of the relation was significantly different from zero

Table 1. Summary of swimbladder dorsal cross-sectional area (mm^2) of anchovies in different physiological states.

	n	Mean	St Dev	min	max
All samples	16	61.36	36.02	24.75	152.17
No Fat	10	74.73	39.76	24.75	152.17
With Fat	6	39.07	9.62	29.67	55.05
Empty stomach	7	60.87	46.15	24.75	152.17
Full stomach	9	61.74	28.90	29.67	111.63

Table 2. Analysis of variance table showing the influence of body weight, depth, HSI, visceral fat, and stomach fill on swimbladder area. Significance codes: P =0 ***, P = 0.001 **, P = 0.01 *.

Response: Area..mm	Df	Sum Sq	Mean Sq	F value	Pr(>F)
Total body weight	1	8251.2	8251.2	19.3339	0.001341 **
Depth	1	2318.1	2318.1	5.4316	0.042009 *
HSI	1	4618.6	4618.6	10.8221	0.008154 **
Visceral fat presence	1	4.8	4.8	0.0113	0.917386
Stomach fill	1	0.0	0.0	0.0001	0.992650
Residuals	10	4267.7	426.8		

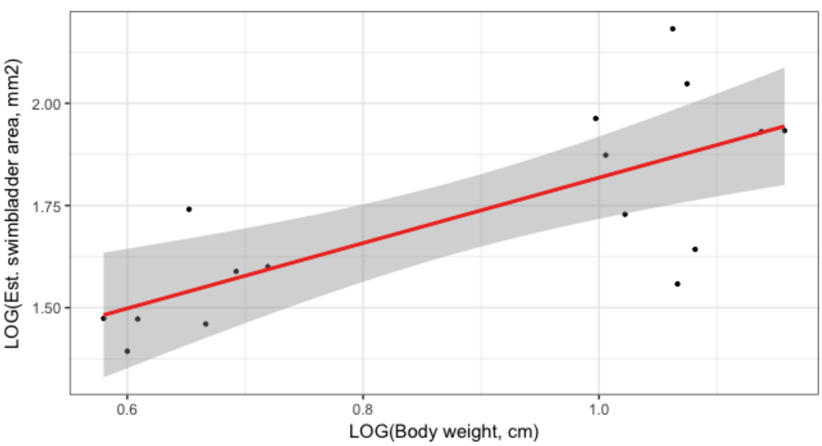

Figure 4. The relationship between swimbladder area and fish size (body length).

Table 3. Effect of length on the swimbladder area. Significance code: P = 0 ***.

Call: lm(log10(Area) ~ log10(length))				
	Estimate	Std. Error	t value	Pr(>|t|)
(Intercept)	1.0184	0.1741	5.849	4.23e-05 ***
log10(TL)	0.7996	0.1916	4.173	0.000939 ***
Multiple R-squared: 0.5543, Adjusted R-squared: 0.5225 F-statistic: 17.41 on 1 and 14 DF, p-value: 0.000939				

and 50% of the variance was explained by the model. The distribution of the residuals of the model representing the relative swimbladder area with length effect removed showed clearly skewed patterns so values were then log-transformed (Figure 5). The transformed distribution, however, was not normal but bimodal. After the length effect was removed, the effects of HSI, presence of visceral fat, stomach fill, and sampling depth on the swimbladder area were reanalyzed. As the output of ANOVA shows, the area of the swimbladder was significantly impacted by the weight of the liver (HSI) and by the depth at which the individuals were sampled (Table 4). The relationships between the relative area and depth and HSI are depicted in Figure 6. As illustrated, the relative area increased with depth and decreased with the size of the liver (HSI).

Among the 207 X-rayed anchovies investigated, 87% of the swimbladders were totally deflated and there were remarkable differences in the swimbladder conditions of anchovies sampled at the same station (Table 5). Only 27 out of 207 individuals had inflated swimbladders and 18 of them were suitable for swimbladder image analysis (Figure 7). According to the approach that considers the shape of the bladder as a series of truncated ellipsoids (Figure 3), the volume ranged between 1.62e-2 cm^3 and 22.29e-2 cm^3, which corresponds to effective radii of 1.57 and 3.76 mm, respectively (Table 6). The effective swimbladder radius distributions of the samples displayed a bimodal pattern in the examined samples (Figure 8). The effects of body weight and sampling depth on the swimbladder volume are presented in Table 7. The effect of weight of the individuals was significant and modeled separately (Table 8). The model estimated effect was removed and the distribution of the residuals is presented in Figure 9. The same figure also displays the log-transformed residuals. The residuals and the transformed residuals were tested to evaluate whether sampling depth had an impact on the relative swimbladder volume (Table 9). The results of both analyses marginally rejected the hypothesis that the effect of depth was significant. The results used to estimate the volume in the "spheroid" approach ranged between 4.09e-2 cm^3 and 446.9e-2 cm^3, which corresponds to effective radii of 0.214 and 0.474 mm, respectively (Table 10). Statistical analysis comparing the volume and the effective radius of the swimbladder calculated by using two shape model approaches (namely "spheroid" and "ellipsoid") showed that both volume and effective radius were significantly

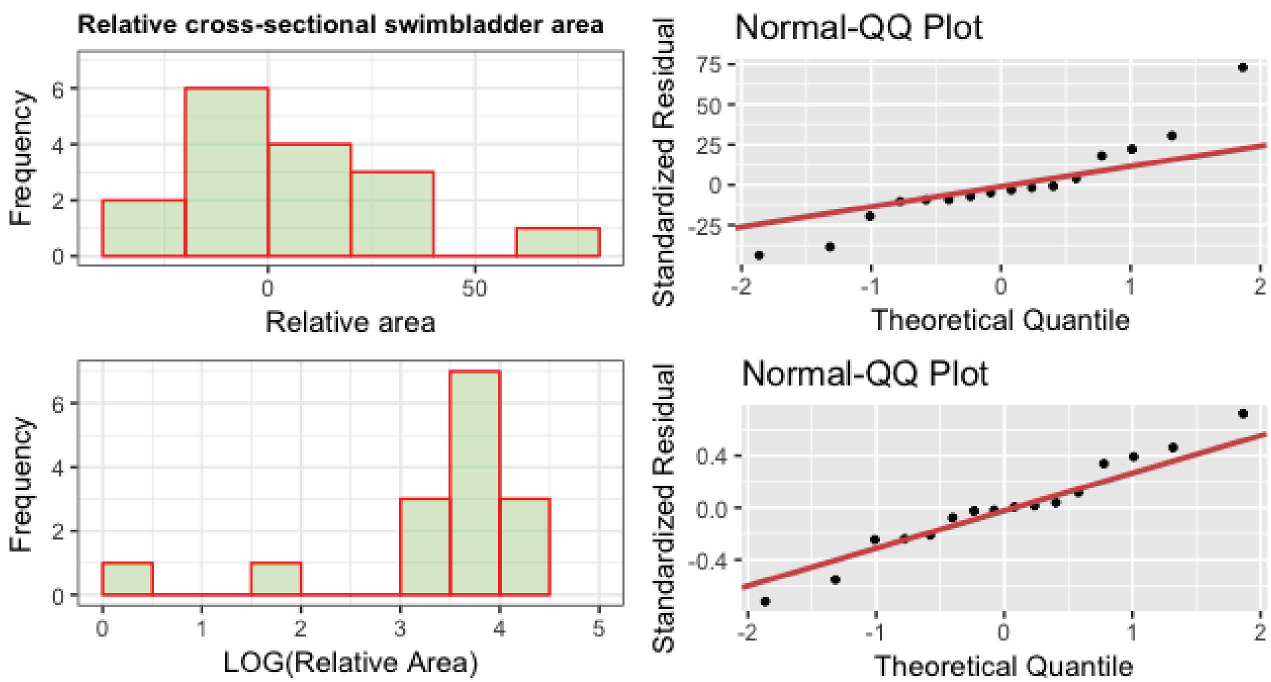

Figure 5. Distribution of the relative cross-sectional area of the sampled anchovies (lower part represents log-transformed values).

Table 4. Analysis of variance table showing the effect of depth, HSI, visceral fat, and Stomach fill on relative swimbladder area. Response: Relative swimbladder area. Significance code: P = 0.01 *.

	Df	Sum Sq	Mean Sq	F value	Pr(>F)
Depth	1	2403.0	2403.0	5.0060	0.04691*
HSI	1	3272.0	3272.0	6.8161	0.02422*
Visceral fat	1	112.0	112.0	0.2333	0.63855
Stomach fill	1	116.5	116.5	0.2428	0.63190
Residuals	11	5280.4	480.0		

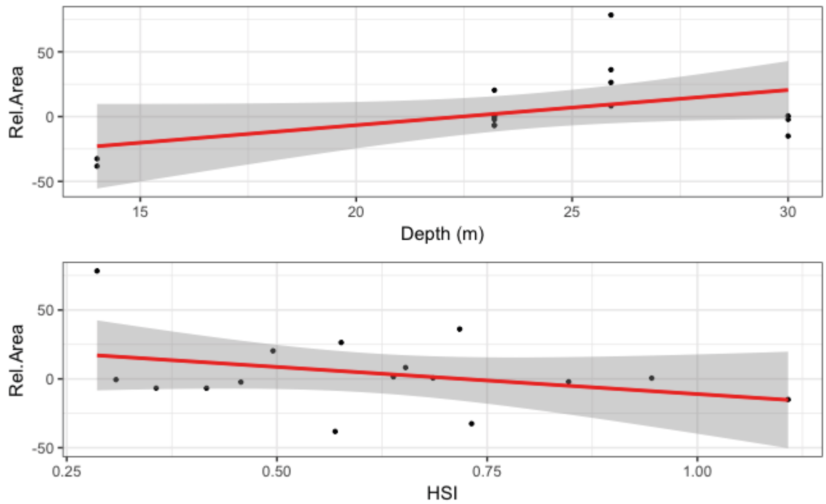

Figure 6. Relationship between relative swimbladder area and depth (upper) and HSI (lower).

Table 5. Condition of the swimbladders of the anchovies sampled.

Station	Deflated	Full	% Full
KD16_007	29	13	31
KD16_014	32	4	11
KD16_024	58	3	5
KD16_036	23	4	15
KD16_038	38	3	7
Total	180	27	13

different ($P < 0.01$). The volume estimated by the spheroid approach is larger than that estimated by the ellipsoid one and the difference in the effective radius estimated by these two methods was 0.088 mm (Figure 10). The theoretic values of TS estimated based on the effective radius of the swimbladder (both "ellipsoid" and "spheroid") and those of conventional estimates are compared in Figure 11. The results of the statistical analysis showed that the slopes of both models were significantly different than 1 (Table 11), indicating that neither of the approaches yielded a TS

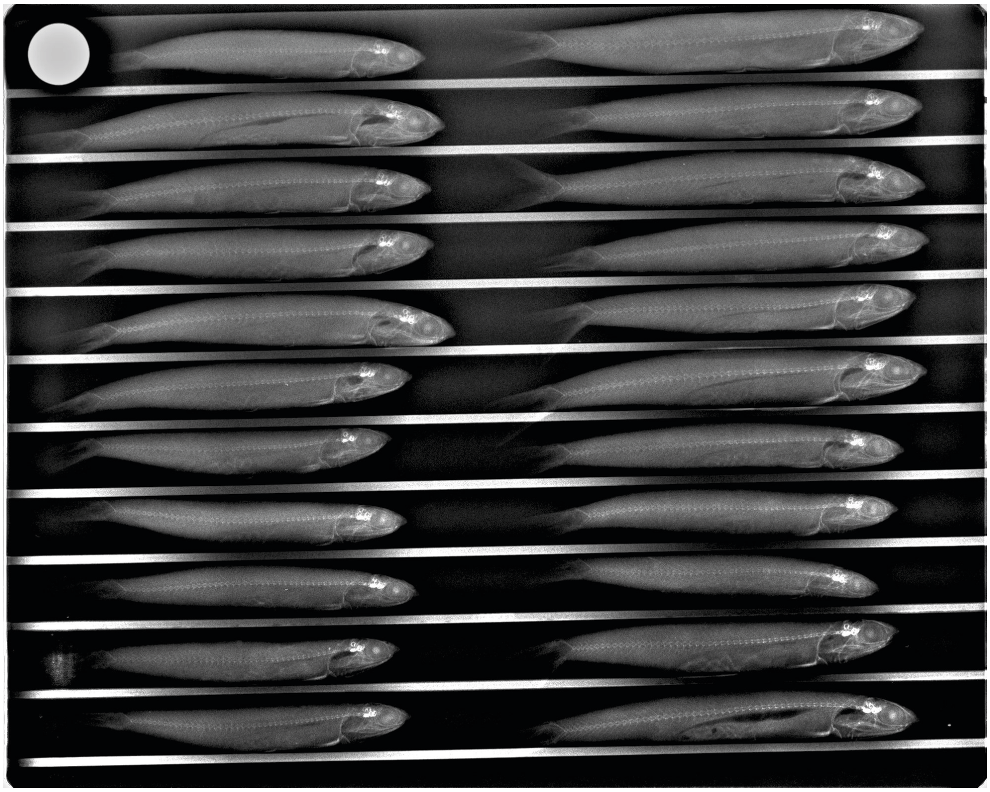

Figure 7. Digitized X-ray image showing individuals having suitable or damaged/deflated swimbladder for image analyses.

Table 6. Volume and effective radius of the swimbladders of the anchovies estimated by ellipsoid approach.

Swimbladder volume (x e-9 m^3)					
Station	Mean	StDev	min	max	n
KD16_007	82.5	57.0	16.2	215.5	13
KD16_014	118.0	96.9	32.0	222.9	3
KD16_038	78.5	27.9	58.8	98.2	2
Total	88.0	60.3	16.2	222.9	18
Effective swimbladder radius (mm)					
KD16_007	2.57	0.61	1.57	3.72	13
KD16_014	2.87	0.90	1.97	3.76	3
KD16_038	2.64	0.32	2.41	2.86	2
Total	2.63	0.61	3.76	18	

estimate similar the conventionally used TS value (b20 = –71.2 dB). Finally, the TS values estimated for ellipsoid and spheroid approaches suggested a b20 value of –90.3 dB and –82.7 dB and these were significantly different than the conventional value of –71.2 dB.

4. Discussion

The results of this study are based on findings from a total of 34 fish, but within the scope of the study, at least ten times more fish were dissected or X-rayed. The reason why such a large part of the samples was disregarded is that

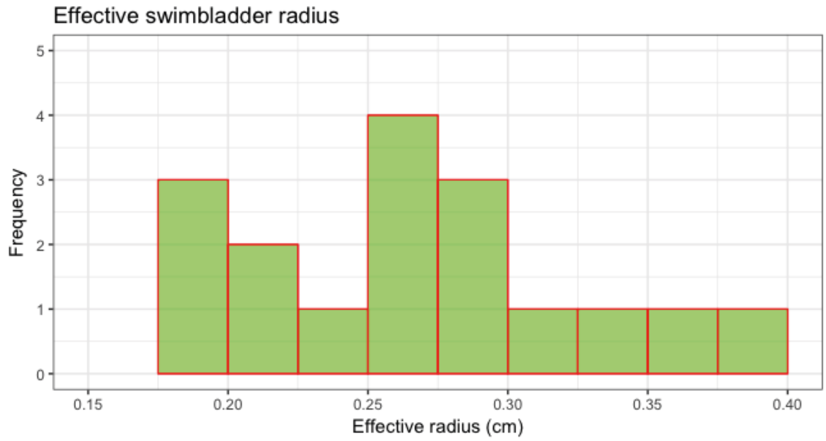

Figure 8. Distribution of the effective swimbladder radius of the sampled anchovies.

Table 7. Analysis of variance table showing the effect of body weight and depth on volume of swimbladder. Significance codes: P = 0.01 *, P = 0.05.

Response: Volume					
	Df	Sum Sq	Mean Sq	F value	Pr(>F)
Body weight.	1	0.017336	0.0173357	7.3709	0.01597*
Depth	1	0.009139	0.0091388	3.8857	0.06744 .
Residuals	15	0.035279	0.0023519		

Table 8. Linear relationship between swimbladder volume and body weight. Significance code: P = 0.01 *.

Call: lm(SB.volume ~ Body weight Residuals				
Min	1Q	Median	3Q	Max
-0.070730	-0.038748	-0.005422	0.019657	0.131615
Coefficients:				
	Estimate	Std. Error	t value	Pr(>|t|)
Intercept	-0.011571	0.041723	-0.277	0.7851
Body weight	0.010256	0.004104	2.499	0.0237*
Residual standard error: 0.05269 on 16 degrees of freedom Multiple R-squared: 0.2807 Adjusted R-squared: 0.2358 F-statistic: 6.245 on 1 and 16 DF, p-value: 0.02373				

these individuals had either totally or partially deflated swimbladders. Unlike the physoclist fishes such as *Trachurus trachurus*, in which inflation and deflation of the swimbladder is controlled through special glands (Alexander, 1993), anchovy is physostomous (Blaxter and Hunter, 1982). The swimbladder in the latter group of fishes is known to be connected to the esophagus and/or digestive tract and so the contents can easily be released when exposed to abnormal conditions, such as pressure difference during sampling or as a stress-response. Although the an-

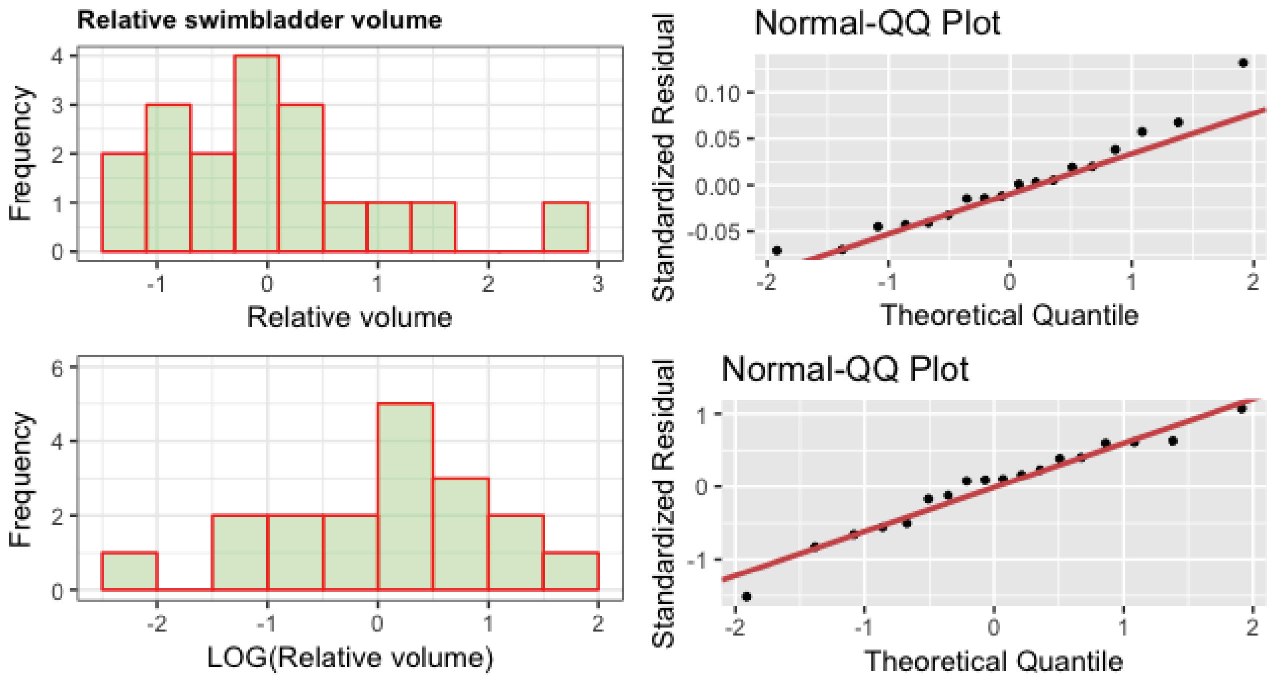

Figure 9. Distribution of residuals of relative volume.

Table 9. Analysis of variance table showing effect of depth on relative volume of swimbladder.

Response: Residuals/Relative volume					
	Df	Sum Sq	Mean Sq	F value	Pr(>F)
Depth	1	3.1316	3.13161	3.4202	0.08297
Residuals	16	14.6501	0.91563		
Response: Log(Residuals) / relative volume					
Depth	1	2.507	2.50698	2.704	0.1196
Residuals	16	14.834	0.92714		

Table 10. Volume and effective radius of the swimbladders of the anchovies estimated by spheroid approach.

Swimbladder volume (x e-9 m^3)					
Station	Mean	StDev	min	max	n
KD16_007	191.3	94.9	52.3	370.5	13
KD16_014	235.0	203.5	40.9	446.9	3
KD16_038	215.4	90.2	151.6	279.2	2
Total	201.3	109.6	40.9	446.9	18
Effective swimbladder radius (mm)					
KD16_007	0.347	0.064	0.232	0.446	13
KD16_014	0.354	0.131	0.214	0.474	3
KD16_038	0.368	0.053	0.331	0.405	2
Total	0.350	0.072	0.214	0.474	18

chovy is a small fish, the relationship between body size and swimbladder area/volume seems to be very important. It is known that a larger swimbladder is needed to neutralize the buoyancy as the size of the fish increases (Jones and Marshall, 1952). A common method used to remove this effect is the use of an isometric/allometric relationship between the swimbladder size and fish length (Machias and Tsimenides, 1996; Ganias et al., 2015). In this study we standardized the swimbladder area and volume by the body weight of the fish. This, we believe, provided a better understanding of the effects of other factors that may be effective on the swimbladder size. As shown by the results of this study, among the effects examined, two were particularly important: the sampling depth and the liver weight (HSI). Two hydrological constraints in the Black Sea, permanent H_2S at depths and sharp vertical temperature gradient, do not allow the anchovy to distribute over a large vertical range. Anchovy schools are usually sighted within the surface layer not exceeding 80 m depth (Gücü et al., 2017). For this reason, the anchovies used in this study were sampled only at depths between 24 and 40 m and the depth interval considered in this study is therefore quite narrow. Depth-dependent swimbladder changes have long been recognized (Ona, 1990) and it is believed to follow Boyle's law, i.e. volume/size of the swimbladder should decrease with depth. Based on direct measurements of swimbladders, several authors described a similar pattern for herring *Clupea herangus* (Blaxter et al.,

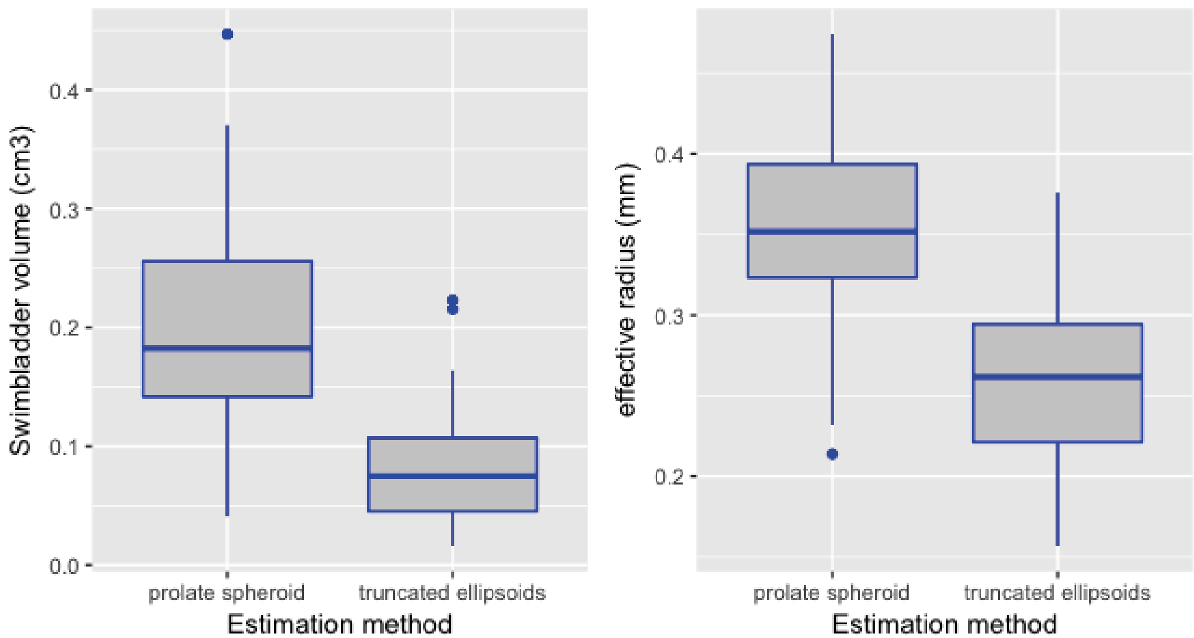

Figure 10. Swimbladder volume and effective radius estimated by two different methods assuming two different shapes.

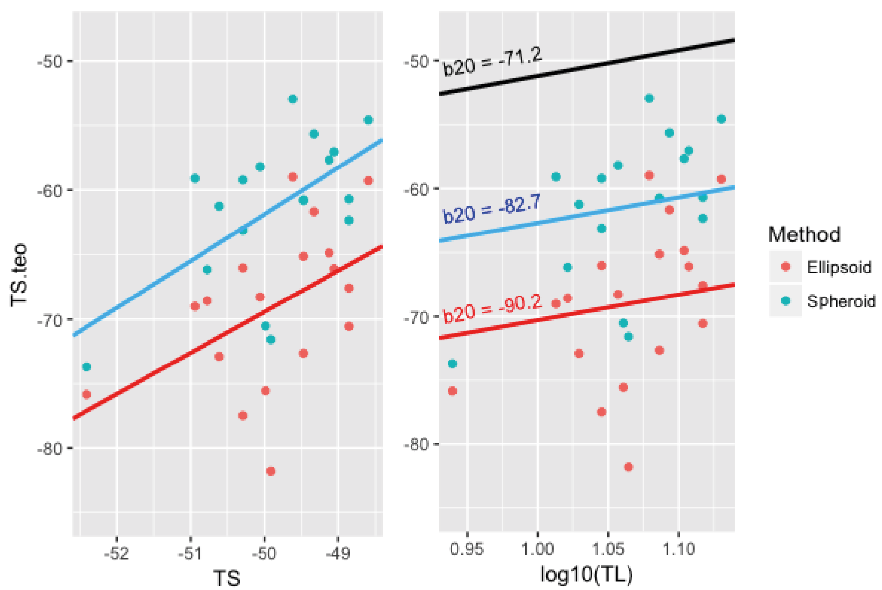

Figure 11. Comparison of the theoretic values of TS estimated based on the effective radius of the swimbladder (both "ellipsoid" and "spheroid") and those of conventional estimates.

1979; Ona, 1990; Fassler et al., 2009) and sardine *Sardina pilchardus* (Ganias et al., 2015). The theory also suggests that the deeper the fish is captured, the larger the swimbladder will be when it is brought from depths (~3 atm) to the surface (~1 atm). This explains the positive relation between swimbladder size and sampling depth observed in this study (Figure 6). Finally, the remarkable difference observed between theoretically estimated b20 values and the one used conventionally for anchovy (Figure 11) indicated that, due to the physostomous nature of the species,

Table 11. Comparison of conventionally estimated TS and theoretically estimated TSs assuming ellipsoid and spheroid shapes. Significance codes: P = 0.01 *, P = 0.05.

lm(TS.teo.ellipsiod ~ TS.b20)				
	Estimate	Std. Error	t value	Pr(>|t|)
Intercept	86.594	70.950	1.220	0.2400
TS	3.184	1.452	2.194	0.0434*
lm(TS.teo.spheroid ~ TS.b20)				
Intercept	115.593	61.126	1.891	0.0769 .
TS	3.622	1.251	2.896	0.0105 *

the quantity of gas escaping out of the swimbladder during operation and handling is significant. For this reason, it is strongly recommended for future studies addressing swimbladder morphology that samples should be acclimatized at a certain pressure until the swimbladder is adapted to the ambient conditions.

This study showed that length-based conventional TS estimates disregarding depth-associated volume changes in the swimbladder and the physiological state of the fishes are prone to noticeable uncertainties in the accuracy of acoustic estimations.

Acknowledgments
The authors gratefully acknowledge financial support from the Office of Naval Research Global, Grant No: N62909-16-1-2092, Ministry of Food, Agriculture, and Livestock, General Directorate of Agricultural Research and Policies, and TÜBİTAK (Project No: KAMAG-110G124. We wish to thank Dr Orest Diachok and Dr Serdar Sakınan, who made valuable suggestions, and the crew of R/V Bilim-2. We are also thankful to Sistem Medical Center and Mezitli Veterinary Clinic for their collaborations on use of their facilities. Finally, we would like to thank the anonymous reviewers, whose contributions are invaluable.

References

Alexander RM (1993). Buoyancy. In: Evans DH, editor. The Physiology of Fishes. Boca Raton, FL, USA: CRC Press, pp. 75-97.

Blaxter JHS, Denton EJ, Gray JAB (1979). The herring swimbladder as a gas reservoir for the acousticolateralis system. J Mar Biol Assoc 59: 1-10.

Blaxter JHS, Hunter JR (1982). The biology of the clupeoid fishes. Adv Mar Biol 20: 1-223.

Fassler SMM, Fernandes PG, Semple SIK, Brierley AS (2009). Depth-dependent swimbladder compression in herring *Clupea harengus* observed using magnetic resonance imaging. J Fish Biol 74: 296-303.

Fassler SMM, O'Donnell C, Jech JM (2013). Boarfish (*Capros aper*) target strength modelled from magnetic resonance imaging (MRI) scans of its swimbladder. ICES J Mar Sci 70: 1451-1459.

Fine ML, McKnight JW Jr, Blem CR (1995). Effect of size and sex on buoyancy in the oyster toadfish. Mar Biol 123: 401-409.

Foote KG (1980). Effect of fish behaviour on echo energy: the need for measurements of orientation distribution. ICES J Mar Sci 39: 193-201.

Foote KG (1985). Rather-high-frequency sound scattering by swimbladdered fish. J Acoust Soc Am 78: 688-700.

Ganias K, Michou S, Nunes C (2015). Field based study of swimbladder adjustment in a physostomous teleost fish. PeerJ 3: e892.

Graham MH (2003). Confronting multicollinearity in ecological multiple regression. Ecology 84: 2809-2815.

Gücü AC, Genç Y, Dağtekin M, Sakınan S, Ak O, Ok M, Aydın İ (2017). On Black Sea anchovy and its fishery. Rev Fish Sci Aquac 25: 230-244.

Hazen EL, Horne JK (2003). A method for evaluating the effects of biological factors on fish target strength. ICES J Mar Sci 60: 555-562.

Hodges RP (2010). Active target strength. In: Hodges RP, editor. Underwater Acoustics: Analysis, Design and Performance of Sonar. 1st ed. Chichester, UK: John Wiley and Sons, pp. 167-183.

ICES (1983). Report of the Planning Group on ICES Coordinated Herring and Sprat Acoustic Surveys. ICES Document CM 1983/H:12. Copenhagen, Denmark: ICES.

Jones HFR, Marshall NB (2008). The structure and function of the teleostean swimbladder. Biol Rev 28: 16-82.

Machias A, Tsimenidis N (1995). Biological factors affecting the swimbladder volume of sardine (*Sardina pilchardus*). Mar Biol 123: 859-867.

Machias A, Tsimenides N (1996). Anatomical and physiological factors affecting the swimbladder cross-section of sardine *Sardina pilchardus*. Can J Fish Aquat Sci 53: 280-287.

MacLennan DN (1990). Acoustical measurement of fish abundance. J Acoust Soc Am 87: 1-15.

Ona E (1990). Physiological factors causing natural variations in acoustic target strength of fish. J Mar Biol Assoc 70: 107-127.

Pena H, Foote KG (2008). Modelling the target strength of *Trachurus symmetricus murphyi* based on high-resolution swimbladder morphometry using an MRI scanner. ICES J Mar Sci 65: 1751-1761.

Pyrounaki MM, Machias A, Giannoulaki M (2012). Target strength equations for anchovy (*Engraulis encrasicolus*) and sardine (*Sardina pilchardus*) from acoustic surveys in Aegean Sea. In: Proceedings of the 10th Panhellenic Symposium of Oceanography and Fisheries; 10–11 May 2012; Athens, Greece. pp. 168-174.

R Core Team (2016). R: A Language and Environment for Statistical Computing. Vienna, Austria: R Foundation for Statistical Computing.

Robertson GN, Lindsey BW, Dumbarton TC, Croll RP, Smith FM (2008). The contribution of the swimbladder to buoyancy in the adult Zebrafish (*Danio rerio*): a morphometric analysis. J Morphol 269: 666-673.

RStudio Team (2017). RStudio: Integrated Development for R. Boston, MA, USA: RStudio, Inc.

Sawada K, Ye Z, Kieser R, Furusawa M (1999). Target strength measurements and modeling of walleye pollock and Pacific hake. Fisheries Sci 65: 193-205.

Scoulding B, Chu D, Ona E, Fernandes PG (2015). Target strengths of two abundant mesopelagic fish species. J Acoust Soc Am 137: 989-1000.

Silva A, Santos M, Caneco B, Pestana G, Porteiro C, Carrera P, Stratoudakis Y (2006). Temporal and geographic variability of sardine maturity at length in the northeastern Atlantic and the western Mediterranean. ICES J Mar Sci 63: 663-676.

Simmonds EJ, MacLennan DN (2005). Fisheries Acoustics: Theory and Practice. 2nd ed. Oxford, UK: Wiley-Blackwell.

Yasuma H, Sawada K, Ohshima T, Miyashita K, Aoki I (2003). Target strength of mesopelagic lanternfishes (family Myctophidae) based on swimbladder morphology. ICES J Mar Sci 60: 584-591.

Zhao X, Wang Y, Dai F 2008. Depth-dependent target strength of anchovy (*Engraulis japonicus*) measured in situ. ICES J Mar Sci 65: 882-888.